Environment International 127 (2019) 190–198

Contents lists available at ScienceDirect

Environment International

journal homepage: www.elsevier.com/locate/envint

Soil lead immobilization by biochars in short-term laboratory incubation studies

Avanthi Deshani Igalavithana[a,1], Eilhann E. Kwon[b,1], Meththika Vithanage[c], Jörg Rinklebe[b,d], Deok Hyun Moon[e], Erik Meers[f], Daniel C.W. Tsang[g], Yong Sik Ok[a,*]

[a] Korea Biochar Research Center, O-Jeong Eco-Resilience Institute & Division of Environmental Science and Ecological Engineering, Korea University, Seoul 02841, Republic of Korea
[b] Department of Environment and Energy, Sejong University, Seoul 05006, Republic of Korea
[c] Office of the Dean, Faculty of Applied Sciences, University of Sri Jayewardenepura, Nugegoda, 10250, Sri Lanka
[d] University of Wuppertal, School of Architecture and Civil Engineering, Institute of Foundation Engineering, Water- and Waste-Management, Soil-and Groundwater-Management, Pauluskirchstraße 7, 42285 Wuppertal, Germany
[e] Department of Environmental Engineering, Chosun University, Gwangju 61452, Republic of Korea
[f] Ghent University, Dept. Green Chemistry & Technology, Faculty of Bioscience Engineering, Coupure Links 653, 9000 Ghent, Belgium
[g] Department of Civil and Environmental Engineering, The Hong Kong Polytechnic University, Hong Kong, China

ARTICLE INFO

Keywords:
CO_2 pyrolysis
Soil stabilization
Metals/metalloids
Waste valorization/recycling
Black carbon
Engineered biochar

ABSTRACT

Exchangeable lead (Pb) extracted by ammonium acetate from three independent incubation studies was assessed to understand the influence of feedstock, pyrolysis temperatures, and production conditions on Pb immobilization capacities of different biochars. Vegetable waste biochar, pine cone, wood bark, cocopeat, red pepper stalk, and palm kernel shell were used as feedstocks (food supply and agricultural wastes) to produce biochars at 200–650 °C with and without N_2/CO_2. Biochars were applied at 5 and 2.5% (w w^{-1}) to a Pb contaminated (i.e., 1445 mg kg^{-1}) agricultural soil collected near an old mine. Lead immobilization in biochar treated soils at the end of incubation period was normalized per gram of biochar applied. Biochar produced from vegetable waste at 500 °C showed the highest Pb immobilization (87%) and highest total exchangeable cations (13.5 $cmol_{(+)}$ kg^{-1}) at the end of the 45 d incubation period. However, on the basis of Pb immobilization per gram of biochar, red pepper stalk biochar produced in CO_2 at 650 °C was the best in Pb immobilization (0.09 mg kg^{-1} g^{-1} biochar) compared to the other biochars. The enhanced ability to immobilize Pb by biochar produced in CO_2 could be due to the presence of siloxanes (−Si−O−Si−) on biochar surface. Pearson correlation analysis revealed that alkaline pH, ash%, and N% of biochars influence in Pb immobilization and exchangeable cation availability in soil. Biochar production atmosphere considerably change its properties that influence Pb immobilization. Further studies are needed on the modification of properties and Pb immobilization by biochars produced from various feedstocks in CO_2.

1. Introduction

Lead (Pb) is a highly toxic metal to both human and animals (Wu et al., 2017). Lead contamination is often reported in soils worldwide due to industrial, mining and agricultural activities (Ahmad et al., 2016a; Beiyuan et al., 2016). Soil Pb contamination has received wide global attention mainly due to high accumulation in plants and the high risk of food chain contaminations. Hence, immobilization measures are essential in contaminated soils to ensure human and animal health (Li et al., 2016).

Biochar has been reported to efficiently immobilize Pb in various soils through a number of distinct mechanisms (Beiyuan et al., 2017; Cui et al., 2016; Li et al., 2013; Moon et al., 2013; Rinklebe et al., 2016). Biochar is a carbon-rich sustainable byproduct of thermal conversion of feedstocks under limited air, or inert (i.e., nitrogen) or reactive atmospheres (i.e., carbon dioxide) (Igalavithana et al., 2018a, 2018b; Lehmann and Joseph, 2009). Changing soil pH to alkaline by biochars is reported by authors as a promising mechanism of soil Pb immobilization (Ahmad et al., 2014a; Zhang et al., 2013). Biochar pH can vary from acidic to alkaline, but is generally reported to be alkaline

* Corresponding author.
E-mail address: yongsikok@korea.ac.kr (Y.S. Ok).
[1] These authors contributed equally to this paper as first authors.

https://doi.org/10.1016/j.envint.2019.03.031
Received 5 December 2018; Received in revised form 12 March 2019; Accepted 12 March 2019
Available online 27 March 2019

Table 1
Physicochemical properties of soil.

Land use	Sand %	Silt %	Clay %	Soil texture	OC[a] %	pH[b]	EC[b] dS m^{-1}	Exchangeable cations				Total
								Ca	K	Mg	Na	Pb
								cmol$_{(+)}$ kg^{-1}	cmol$_{(+)}$ kg^{-1}	cmol$_{(+)}$ kg^{-1}	cmol$_{(+)}$ kg^{-1}	mg kg^{-1}
Fallowed upland agriculture (Igalavithana et al., 2017a)	79.9	9.2	10.8	sandy loam	5.8	4.9	0.1	0.1	0.04	0.04	0.01	1445

Soil contamination warning limit Korea (Ministry of Environment Korea, 2016).
[a] Organic carbon.
[b] 1:5 soil to deionized water ratio.

(Igalavithana et al., 2018a). The high pH values of biochar increase the soil pH and decrease the mobility of Pb in contaminated soils (Igalavithana et al., 2017a). The exchange of Pb^{2+} ions with other cations (e.g., Ca^{2+}, K^{+}, Na^{+}, Mg^{2+}) in biochars is another significant mechanism of Pb immobilization (Ho et al., 2017; Wang et al., 2015). Ion exchange enhances the binding of Pb on biochar surfaces and significantly reduces its mobility (Ho et al., 2017). Moreover, Pb precipitation with common anions (e.g., PO_4^{3-}, OH^{-}, Cl^{-}) and the formation of stable Pb compounds such as hydroxyl pyromorphite on biochar surfaces is identified as a vital mechanism of Pb immobilization (Ho et al., 2017; Igalavithana et al., 2017a). In addition, Wang et al. (2017) observed surface complexation with functional groups (e.g., −OH, −COOH, −CH, −C═O, C═C) as one of the main mechanisms of Pb immobilization by biochar in soils. Similarly, Vamvuka et al. (2018) also reported the huge capacity of surface functional groups of biochars in Pb immobilization. Furthermore, the electrostatic attraction between biochar and Pb has considerable impact on soil Pb immobilization (Igalavithana et al., 2018b; Shen et al., 2018). Several authors have reported electrostatic attraction as an important mechanism to reduce the Pb mobility in contaminated soils (Ahmad et al., 2016b; Mahmoud et al., 2018). Biochar Pb immobilization mechanisms depend on the biochar properties such as pH, ash content, aromaticity, surface area, and surface functional groups. The dominant Pb immobilization mechanisms for each biochar vary with their properties (O'Connor et al., 2018; Rajapaksha et al., 2016). Biochar properties depend on the feedstock materials, pyrolysis conditions and pre- and post-treatments (Igalavithana et al., 2018a).

Various feedstocks are used to produce biochar, and continuously testing the new feedstocks such as food wastes for biochar production (Gupta et al., 2018; Igalavithana et al., 2018a). The pH and ash content are high in biochars produced from manure as it contains a high amount of minerals (Meier et al., 2015). In general, biochars produced from woody feedstocks were reported to have high surface areas due to their inherent porous structures (Abdel-Fattah et al., 2015). Biochar surface functional groups are highly heat sensitive, hence, amount of surface functional groups reduced with increased pyrolysis temperature (Igalavithana et al., 2017a). However, biochar surface area, porosity, pH, EC, and aromaticity increased with the increasing pyrolysis temperature (Igalavithana et al., 2018a; Novak et al., 2009). Pre- and post-treatments to alter biochar properties are routinely used to enhance performance in different ways including Pb immobilization (Arabyarmohammadi et al., 2018; Rajapaksha et al., 2016).

Scientists are continuously studying the efficiency of biochars for soil Pb immobilization in the short and long terms, with a focus on long-term immobilization. Even though the short term Pb immobilization data might not provide clear evidence of the long term impacts, the short-term effectiveness of biochar can help identify potential amendments for long term evaluation. Hence, short term Pb immobilization potential in a contaminated agricultural soil by eleven biochars produced from vegetable wastes, pine cone, and crop residues at 200, 500 and 650 °C was tested under laboratory conditions. Three independent laboratory incubation studies were conducted under comparable experimental conditions and observed dissimilar Pb immobilization by different biochars (Igalavithana et al., 2017a, 2017b, 2018b). Therefore, this study was conducted: 1) to find out the best biochar in term of short term Pb immobilization, 2) to evaluate the most important biochar properties influencing Pb immobilization, 3) to understand the impact of biochars on soil nutrient status (i.e., exchangeable cations). In order to achieve the above objectives, exchangeable Pb and exchangeable cations extracted with ammonium acetate (NH_4OAc, 1 M, pH 7) in the soil after the incubation period of three independent incubation studies were statistically evaluated.

2. Material and methods

2.1. Studied data

Data were obtained from three laboratory incubation studies (LIS-1, LIS-2, LIS-3) conducted to evaluate Pb immobilization in a contaminated soil by biochars (Igalavithana et al., 2017b, 2017a, 2018b). The soil was sampled from fallowed agricultural lands located near a historical mining area that reported with high levels of Pb (i.e., 1445 mg kg^{-1}), exceeding the Korean soil contamination warning limits (Ministry of Environment Korea, 2016). Physicochemical properties of the test soil are listed in Table 1. The soil belonged to the sandy loam textural class as per the USDA soil textural classification. Soil pH was acidic (i.e., 5.1).

Eleven biochars were used in three laboratory soil incubation studies (Table 2). Pine cone, vegetable waste and vegetable waste + pine cone (1:1) biochars produced at 200 °C and 500 °C pyrolysis temperatures (P200, P500, V200, V500, PV200 and PV500) were used in LIS-1. Pyrolysis temperature was achieved at a 7 °C min^{-1} heating rate, and held at the maximum temperature for 2 h. Biochars were produced under limited oxygen (O_2) in covered crucibles in a muffle furnace (Igalavithana et al., 2017a). Biochars used in LIS-2 were produced from wood bark, cocopeat and palm kernel shell were produced under pyrolysis conditions of heating temperature 500 °C, heating rate 10 °C min^{-1}, and a holding time 1 h, and nitrogen (N_2) purging rate 1.5 L min^{-1} (WB, CP and PKS, respectively) (Lee et al., 2013). In LIS-3 red pepper stalk biochar was produced at 650 °C by purging N_2 or carbon dioxide (CO_2) at rates of 0.5 L min^{-1} (RPS-N and RPS-C) (Lee et al., 2017). All the biochars were produced by slow pyrolysis heating programs.

Moisture, mobile matter (or volatile matter or labile matter), and ash content of biochars were determined as explained in Ahmad et al. (2012c) at 105, 450 and 750 °C using a muffle furnace (LT, Nabertherm, Germany), and resident matter (or fixed matter) was calculated as explained in Igalavithana et al. (2018a). The elemental composition (i.e., C, H, O, and N) of biochars were analyzed using an elemental analyzer (EuroEA, EA, Italy). A ratio of 1 g: 20 mL soil-to-deionized water was used to determine biochar pH and EC (Inyang et al., 2012). Biochar surface area was calculated using the Brunauer–Emmett–Teller (BTE)

Table 2
Biochar production conditions.

Biochar	Production method	Pyrolysis temperature °C	Heating rate °C min^{-1}	Holding time h	Purged gas	Purging rate L min^{-1}
V200[a]	Slow pyrolysis	200	7	2	–	–
P200[a]	Slow pyrolysis	200	7	2	–	–
PV200[a]	Slow pyrolysis	200	7	2	–	–
V500[a]	Slow pyrolysis	500	7	2	–	–
P500[a]	Slow pyrolysis	500	7	2	–	–
PV500[a]	Slow pyrolysis	500	7	2	–	–
WB[b]	Slow pyrolysis	500	10	1	N_2	1.5
CP[b]	Slow pyrolysis	500	10	1	N_2	1.5
PKS[b]	Slow pyrolysis	500	10	1	N_2	1.5
RPS-N[c]	Slow pyrolysis	650	10	1	N_2	0.5
RPS-C[c]	Slow pyrolysis	650	10	1	CO_2	0.5

V, Vegetable waste; P, Pine cone; PV, Vegetable waste + Pine cone (1:1); WB, Wood bark; CP, Cocopeat; PKS, Palm kernel shell; RPS, Red pepper stalk.
[a] Igalavithana et al. (2017a).
[b] Lee et al. (2013).
[c] Lee et al. (2017).

method, and the average pore volume and diameter were calculated using the Barret–Joyner–Halender (BJH) method using nitrogen adsorption-desorption isotherms.

Biochar application rates were 5% (w w^{-1}) in LIS-1 and LIS-2, and 2.5% (w w^{-1}) for LIS-3. Biochar was mixed well with soil, and the soil water content was maintained at 70% water holding capacity during the incubation period. Incubation was carried in an incubator (MIR-554, SANYO Electronic, Co., Ltd., Tokyo, Japan) at 25 °C. LIS-1 and LIS-2 soils were incubated for 45 days, and 30 days for the LIS-3. When considering the incubation conditions, only the number of days and the biochar application rates were different in LIS-1, LIS-2 and LIS-3.

Ammonium acetate (NH_4OAc, 1 M, pH 7, 1:10; soil to solution) extractable Pb concentrations in biochar treated and control soils after the incubation period of LIS-1 were determined, and previously determined NH_4OAc extractable Pb in LIS-2 and LIS-3 were considered in this study to evaluate the biochar performance in Pb immobilization. Ammonium acetate extracts weakly bound and exchangeable Pb that can be easily released and mobilized (Anjos et al., 2012; Ure, 1996). Moreover, acetate prevents the reabsorption and precipitation of released Pb ions (Ure, 1996). As weakly bound and exchangeable Pb are generally considered the mobile fractions, NH_4OAc extraction was used to evaluate the Pb immobilization capacity of the biochar treatments. Also, exchangeable cations extracted from 1 M NH_4OAc at pH 7 and measured using an inductively coupled plasma optical emission spectrophotometer (ICP-OES; Optima 7300 DV, Perkin-Elmer, USA) were used to assess the effect of biochar on soil cation availability. Soil pH and electrical conductivity (EC) values determined in 1:5 soil to deionized water ratio were also monitored (Igalavithana et al., 2018b, 2017b, 2017a). Three replicates were used for all the analyses, and the instruments were calibrated after every ten samples.

2.2. Data analysis

Data obtained from three independent laboratory incubation studies were analyzed without data normalization by using one-way analysis of variance (ANOVA) and Tukey's honestly significant difference (HSD) test at probability (p) level of < 0.05. Lead immobilization percentage in biochar treated soil was calculated relative to the control for each respective study. Lead immobilization by biochar was further analyzed to remove the differences in biochar application rates. Immobilization of Pb in each treatment was calculated as mg kg^{-1} g^{-1} biochar relative to the respective control.

Calculated data were statistically analyzed (ANOVA and HSD) to understand the biochar capacity to immobilize Pb in the soil. Pearson correlation analysis (Pearson correlation coefficient: r) was conducted among all obtained and calculated data, and soil and biochar properties. SAS statistical software was employed for ANOVA, HSD, and Pearson correlation analyses (SAS, Cary, NC, USA).

Normal distribution of calculated Pb immobilization data (i.e., percentage and mg kg^{-1} g^{-1} biochar) was analyzed using Minitab 16 statistical software at 95% confident interval (CI). Principal component analysis (PCA) evaluating biochar treatment properties (i.e., soil pH and EC, NH_4OAc extractable Pb, calculated Pb immobilization values, biochar application rate and incubation period) was conducted using the same statistical software.

3. Results and discussion

3.1. Biochar properties

Biochar carbon can be classified into two groups as mobile matter (or volatile matter or labile matter) and resident matter (or fixed matter) based on their stability. Mobile matter mainly consists of aliphatic and small aromatic carbon structures, and resident matter consists of large aromatic carbon structures (Ahmad et al., 2012b; Mia et al., 2017). Mobile matter content in biochars decreased with increasing pyrolysis temperature from low temperature (i.e., 200 °C) to high temperatures (i.e., 500 and 650 °C) as expected. The highest mobile matter contents were found in P200, PV200, and V200 (i.e., 62.35, 58.37 and 56.44%), and the lowest were reported in P500 and PV500 (i.e., 10.01 and 10.33) (Table 3). Resident matter (or fixed matter), ash and carbon (C) contents in biochars increased with increasing pyrolysis temperature. The highest and lowest resident matter (or fixed matter) contents were detected in PKS and V200 (i.e., 80.85% and 25.76%) respectively. The V500 (36.67%) had the highest ash content, and P200 had the lowest (i.e., 0.77%). The carbon content in biochars produced at 500 and 650 °C was > 80% except in V500 and P500. Those two biochars showed higher oxygen (O%) (i.e., V500: 16.81% and P500: 20.94%) than the other biochars produced at 500 and 650 °C, which had O% in a range of 8.14–11.36%. However, O% in V500 and P500 was lower than the V200 and P200 (i.e., 36.02 and 27.09%) which were produced from same feedstocks at low temperature (i.e., 200 °C).

A Van Krevelen diagram of the studied biochars (Fig. 1) showed very low O/C and H/C ratios in PV500, CP, WB, PKS, RPS-N and RPS-C, which corresponds to the high dehydrogenation and deoxygenation from feedstock during the biochar production (Van Poucke et al., 2015). The V500 showed high dehydrogenation and deoxygenation compared to the V200. However, P500 did not show a significant reduction in O/C and H/C ratios compared to the P200. Decreased H/C and O/C ratios indicate an increase of aromaticity in biochar and a reduction of surface polarity (Wiedner et al., 2013; Xiao et al., 2016). The International Biochar Initiative (IBI) suggests a maximum value for

Table 3
Biochar properties.

Biochar	Pyrolysis temp. °C	Purged gas	Moisture %	Mobile matter (volatile matter) %	Resident matter (fixed matter) %	Ash %	C[d] %	H[d] %	N[d] %	O[d] %	H/C	O/C	pH[e]	EC[e] dS m^{-1}	Surface area[f] $m^2 g^{-1}$	APV[g] $\times 10^{-3} m^3 g^{-1}$	APD[g] nm
V200[a]	200	–	1.20	56.44	25.76	16.59	52.89	6.90	4.20	36.02	1.56	0.51	5.95	0.041	0.36	2.59	43.24
P200[a]	200	–	1.27	62.35	35.60	0.77	69.74	2.13	1.03	27.09	0.37	0.29	4.15	0.001	0.47	2.38	45.13
PV200[a]	200	–	1.00	58.37	32.72	7.91	54.66	5.91	0.57	38.85	1.30	0.53	5.26	0.000	0.44	0.43	23.27
V500[a]	500	–	0.72	12.43	50.17	36.67	74.71	3.08	5.41	16.81	0.49	0.17	11.23	0.121	1.16	2.42	22.80
P500[a]	500	–	1.42	10.01	79.60	8.96	74.64	2.62	1.81	20.94	0.42	0.21	6.77	0.001	192.97	10.2	2.44
PV500[a]	500	–	1.07	10.33	70.53	18.06	83.85	2.70	3.71	9.73	0.39	0.09	10.39	0.045	50.26	3.22	54.61
WB[b]	500	N_2	0.36	18.14	68.66	12.84	84.84	3.13	1.83	10.20	0.44	0.09	9.6	–	13.6	–	109.9
CP[b]	500	N_2	2.55	14.30	67.25	15.90	84.44	2.88	1.02	11.67	0.41	0.10	10.3	–	13.7	–	24,310
PKS[b]	500	N_2	0.00	12.29	80.85	6.86	87.85	2.91	1.11	8.14	0.40	0.07	6.9	–	191	–	57.2
RPS-N[c]	650	N_2	2.52	22.04	66.14	9.30	86.63	2.42	2.62	8.34	0.33	0.07	12.19	0.20	32.46	0.02	3.79
RPS-C[c]	650	CO_2	3.33	22.71	62.05	11.91	83.85	2.22	2.56	11.36	0.32	0.10	9.50	0.11	109.15	0.09	2.64

V, Vegetable waste; P, Pine cone; PV, Vegetable waste + Pine cone (1:1); WB, Wood bark; CP, Cocopeat; PKS, Palm kernel shell; RPS, Red pepper stalk.
APV, average pore volume; APD, average pore diameter.
[a] Igalavithana et al. (2017a).
[b] Lee et al. (2013).
[c] Lee et al. (2017).
[d] Moisture and ash free.
[e] 1:20 ratio of biochar to deionized water.
[f] Brunauer-Emmett-Teller (BTE) method.
[g] Barret-Joyner-Halender (BJH) method.

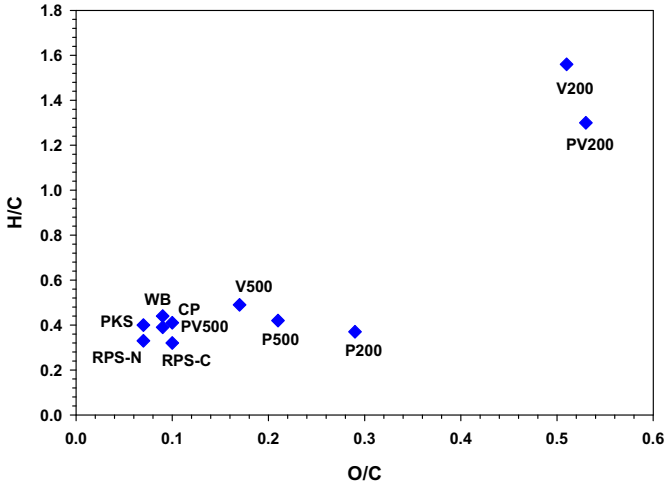

Fig. 1. Van Krevelen diagram for considered biochars. H/C and O/C ratio were obtained from Table 3. V, Vegetable waste; P, Pine cone; PV, Vegetable waste + Pine cone (1:1); WB, Wood bark; CP, Cocopeat; PKS, Palm kernel shell; RPS, Red pepper stalk. 200 and 500 denote the pyrolysis temperatures of 200 and 500 °C. −N and −C represent the purged gas of N_2 and CO_2. (For interpretation of the references to colour in this figure legend, the reader is referred to the web version of this article.)

the H/C ratio in biochar of 0.7, but there is no limit for O/C ratio (IBI, 2015). Hence, V200 and PV200 which have > 0.7 H/C ratios cannot be considered as biochars, and we reported them as torrefied biomass in our previous study (Igalavithana et al., 2017a). In contrast, P200 can be considered as a biochar according to the IBI regulation even though the pyrolysis temperature was very low (i.e., 200 °C).

Biochar pH increased with increasing pyrolysis temperature, and V500, PV500, WB, CP, RPS-N and RPS-C had alkaline pH values in a range of 9.5–12.19. The remaining biochars had neutral or acidic pH values in the range of 4.15–6.90. The RPS-N and P200 had the highest and lowest pH values of 12.19 and 4.15, respectively. High pyrolysis temperatures increased the ash content in biochar which is responsible for the high pH (McBeath et al., 2014). High-temperature biochar can be beneficial in acidic soil applications to increase the soil pH (Lehmann and Joseph, 2009). The P500, PKS and RPS-C had the highest surface areas respectively as 193, 191, and 109 $m^2 g^{-1}$. The highly porous structures in pine cone and palm kernel shell may have opened at a comparatively high pyrolysis temperature of 500 °C due to the volatilization of mobile matter (Igalavithana et al., 2017a). The CO_2 induced reactions with tar enhanced the pore spaces in the RPS-C biochar (Lee et al., 2017).

3.2. Lead immobilization

All biochars except P200 and P500 decreased the NH_4OAc extractable Pb in soil compared to the control (Fig. 2a). Application of P200 (i.e., 5%) increased the NH_4OAc extractable Pb in soil while P500 did not show significant difference with the control (C1). The V500 showed the lowest concentration of NH_4OAc extractable Pb (i.e., 0.47 mg kg^{-1}) followed by RPS-C and WB (i.e., 1.21 and 1.23 mg kg^{-1}).

Increased pH in soil (Table 4) due to biochar application might be the main mechanism for the reduced NH_4OAc extractable Pb in soil. The Pearson correlation analysis supported those results; NH_4OAc extractable Pb and soil pH showed a strong negative correlation ($r = -0.9428$, $p < 0.0001$). When increasing the soil pH, the density of negatively charged sites in soils also increases, which may have facilitated immobilization of the cationic Pb (Pb^{2+}) in soil (Ahmad et al., 2012a). In addition, biochar ash and N% showed negative correlations to the NH_4OAc extractable Pb (ash: $r = -0.7866$, $p = 0.0041$; N%: $r = -0.6674$, $p = 0.0248$). Biochar ash might have induced the co-precipitation of Pb with cations and anions such as Ca^{2+}, Mg^{2+}, PO_4^{3-} (Ahmad et al., 2014b; Liang et al., 2014; Park et al., 2011). Nitrogen containing surface functional groups, amine (-NH_2) in particular, might have facilitated Pb immobilization by strong covalent bonding. The presence of amino groups on the biochar surface increases the number of cation exchangeable sites (Singh et al., 2015). Yang and Jiang (2014) observed enhanced Cu^{2+} adsorption by biochar due to the increased –NH_2 surface functional groups by amino modification. None of the other biochar properties showed any significant correlation to the NH_4OAc extractable Pb in the soil.

The highest Pb immobilization percentage was accomplished by the V500 application (i.e., 87.0%), followed by WB, RPS-C and PV500 with 66.1, 64.5 and 62.6% of Pb immobilization, respectively (Fig. 2b).

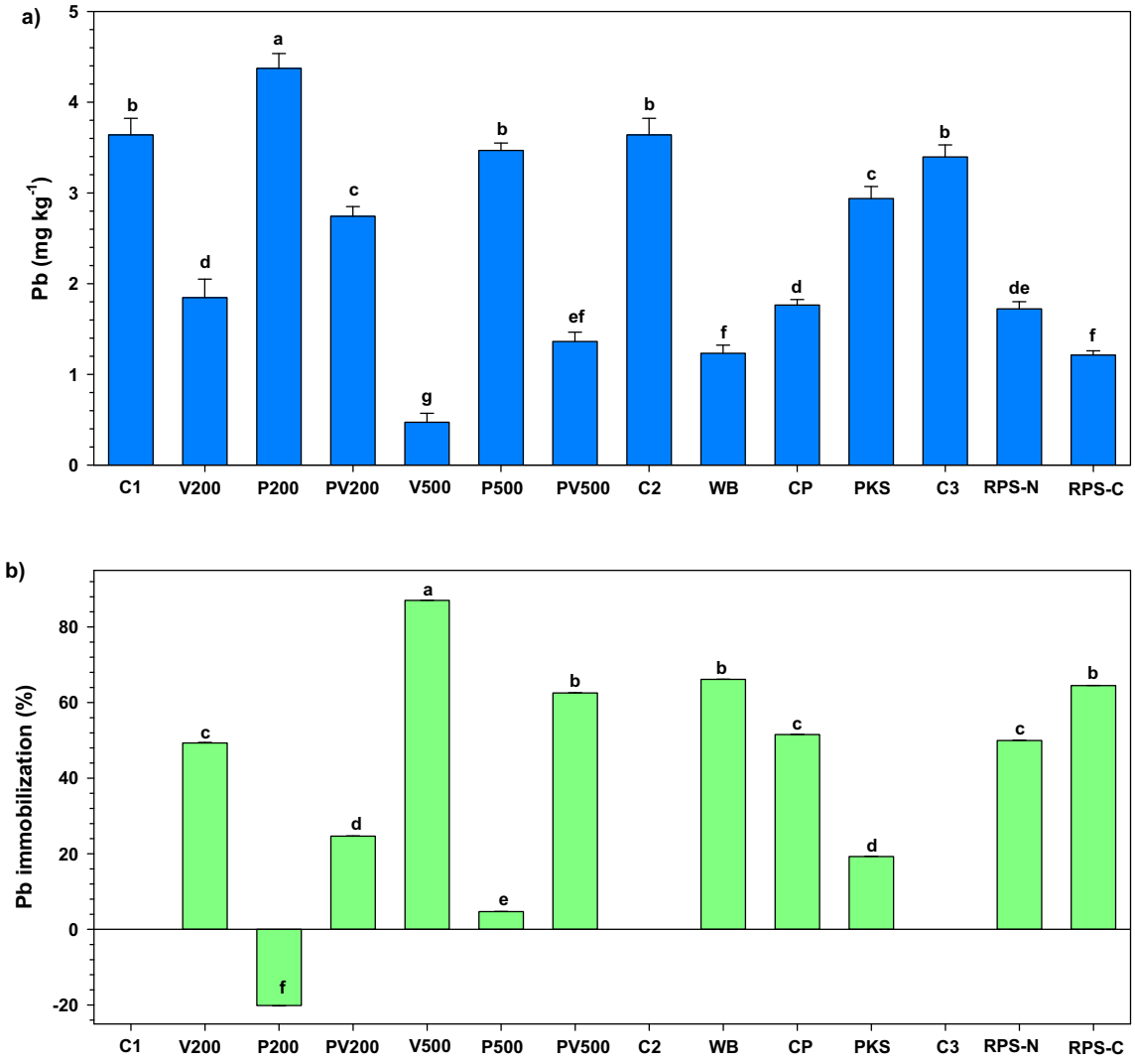

Fig. 2. NH_4OAc extractable Pb (a) and Pb immobilization percentage compare to the control (b) in soil after the incubation period. V, Vegetable waste; P, Pine cone; PV, Vegetable waste + Pine cone (1:1); WB, Wood bark; CP, Cocopeat; PKS, Palm kernel shell; RPS, Red pepper stalk. 200 and 500 denote the pyrolysis temperatures of 200 and 500 °C. −N and −C represent the purged gas of N_2 and CO_2. C1, C2 and C3 are the controls of LIS1, LIS2 and LIS3. Vertical lines on bars represent the standard deviation. Different letters above the bars represent the statistically significant differences at $p < 0.05$ (Tukey's HSD test). (For interpretation of the references to colour in this figure legend, the reader is referred to the web version of this article.)

However, when considering the Pb immobilization per gram of biochar applied, RPS-C obtained the highest capacity, followed by the RPS-N and V500 (Fig. 3). Even though the V500 showed the highest immobilization percentage of Pb at the end of the incubation period, the biochar application rate of V500 to soil was 5%, but it was 2.5% for RPS-N and RPS-C. Normalized data clearly demonstrated that RPS-C has the highest capacity to immobilize Pb in soils, followed by RPS-N and V500 (Fig. 3). We observed oxygen-containing functional groups of aldehydes (−C−C═O) and siloxanes (−Si−O−Si−) on RPS-C surface but not on RPS-N surface in our previous study (Igalavithana et al., 2018b). The enhanced ability of RPS-C to immobilize Pb might be due to the presence of siloxanes which have a higher affinity to retain cationic metals.

The NH_4OAc extractable Pb was increased in the P200 treatment (Fig. 3). Obviously, Pb cannot be retained by this biochar in comparison to the control. Possible reasons for this can be the comparatively low pH of P200 (i.e., 4.15) (Yin et al., 2016). In addition, the leached Pb might be associated with dissolved organic matter (DOM) via complexation as described earlier by Weng et al. (2002). Li et al. (2013) observed Pb complexation with DOM in the rhizosphere and increased mobility. However, the PV200 treatment, produced from incorporating vegetable waste at a 1:1 ratio with pine cone at a pyrolysis temperature of 200 °C, showed significant Pb immobilization in the soil. The high soil pH increase (i.e., 6.52) and ash content (i.e., 16.6%) of V200 compared to the P200 might be the reason for the high Pb immobilization. Hence, this suggests the ability to improve Pb immobilization capacity by blending feedstock materials (e.g., vegetable waste) before pyrolysis. This is an important finding in biochar production for cationic metal immobilization in soil. Further studies are needed to understand the mechanisms.

Biochars produced at high temperatures always showed higher Pb immobilization than those produced at low temperatures (Fig. 3). When considering the feedstock, production of biochar from red pepper stalk, vegetable waste, vegetable waste + pine cone (1:1) and wood bark might be more beneficial in immobilizing soil Pb, which showed the highest Pb immobilization capacity as observed in the current study. Moreover, biochar production in CO_2 at 650 °C provided an enhanced capacity of Pb immobilization, presumably due to the high surface area, pH and surface functional groups, and formation of new surface functional groups of siloxane compared to the biochar produced at 650 °C in N_2 from red pepper stalk. Moreover, biochar produced in CO_2 increases the aromatic carbon structures more than the biochars produced in N_2

Table 4
Soil chemical properties after the incubation period. Data represent as mean (standard deviation). Different letters after the parentheses represent the statistically significant differences at $p < 0.05$ (Tukey's HSD test).

	Biochar	K	Ca	Mg	Na	Total (sum of K, Ca and Mg)	pH[d]	EC[d]
		$cmol_{(+)}\,kg^{-1}$	$cmol_{(+)}\,kg^{-1}$	$cmol_{(+)}\,kg^{-1}$	$cmol_{(+)}\,kg^{-1}$	$cmol_{(+)}\,kg^{-1}$		$dS\,m^{-1}$
LIS-1	C1[a]	0.44 (0.01) f	1.63 (0.07) gh	0.61 (0.03) g	0.03 (0.00) e	2.68 (0.12) f	5.01 (0.00) f	0.12 (0.00) ef
	V200[a]	4.61 (0.08) b	2.95 (0.01) c	1.90 (0.03) a	1.03 (0.00) b	9.46 (0.08) b	6.52 (0.22) bcd	0.98 (0.05) b
	P200[a]	0.47 (0.00) f	1.96 (0.03) ef	0.70 (0.01) ef	0.03 (0.00) e	3.13 (0.05) f	5.30 (0.03) ef	0.06 (0.01) e
	PV200[a]	2.25 (0.03) d	2.41 (0.05) d	1.25 (0.00) c	0.48 (0.02) d	5.91 (0.04) d	5.96 (0.05) de	0.42 (0.01) d
	V500[a]	9.05 (0.12) a	2.90 (0.03) c	1.53 (0.07) b	1.81 (0.03) a	13.48 (0.19) a	7.97 (0.26) a	2.02 (0.02) a
	P500[a]	0.51 (0.01) f	1.83 (0.04) fg	0.63 (0.01) fg	0.04 (0.00) e	2.96 (0.06) f	5.24 (0.01) f	0.09 (0.00) ef
	PV500[a]	4.45 (0.36) b	2.14 (0.12) de	0.90 (0.04) d	0.60 (0.05) c	7.49 (0.42) c	6.76 (0.24) bc	0.78 (0.05) c
LIS-2	C2[b]	0.44 (0.01) f	1.63 (0.07) gh	0.61 (0.03) g	0.03 (0.00) e	2.68 (0.12) f	5.01 (0.00) f	0.12 (0.00) ef
	WB[b]	1.07 (0.00) e	4.11 (0.02) a	0.72 (0.01) e	0.03 (0.00) e	5.91 (0.03) d	6.91 (0.17) bc	0.14 (0.00) e
	CP[b]	3.54 (0.17) c	1.43 (0.05) h	0.57 (0.02) g	1.75 (0.08) a	5.53 (0.23) de	6.32 (0.57) cd	0.79 (0.03) c
	PKS[b]	0.56 (0.03) f	1.61 (0.11) gh	0.57 (0.03) g	0.03 (0.00) e	2.74 (0.18) f	5.38 (0.34) ef	0.06 (0.00) e
LIS-3	C3[c]	0.43 (0.03) f	1.74 (0.10) fg	0.56 (0.03) fg	0.02 (0.00) e	2.77 (0.16) f	5.11 (0.02) f	0.12 (0.01) ef
	RPS-N[c]	0.99 (0.04) e	3.69 (0.20) b	0.63 (0.04) g	0.04 (0.00) e	5.31 (0.29) e	6.57 (0.02) bcd	0.13 (0.00) ef
	RPS-C[c]	1.06 (0.02) e	4.26 (0.12) a	0.61 (0.01) g	0.05 (0.00) e	5.93 (0.15) d	7.00 (0.06) b	0.13 (0.01) e

LIS, Laboratory incubation study.
V, Vegetable waste; P, Pine cone; PV, Vegetable waste + Pine cone (1:1); WB, Wood bark; CP, Cocopeat; PKS, Palm kernel shell; RPS, Red pepper stalk, C1, Control 1; C2, Control 2 and C3, Control 3.
[a] Igalavithana et al. (2017a).
[b] Igalavithana et al. (2017b).
[c] Igalavithana et al. (2018b).
[d] 1:5 soil to deionized water ratio.

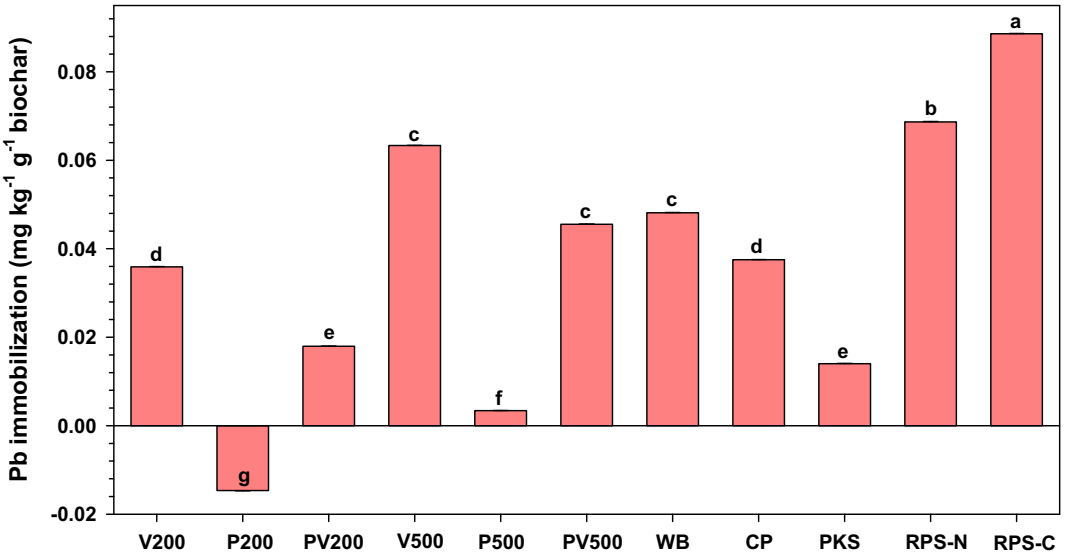

Fig. 3. Pb immobilization per gram biochar in soil after the incubation period. V, Vegetable waste; P, Pine cone; PV, Vegetable waste + Pine cone (1:1); WB, Wood bark; CP, Cocopeat; PKS, Palm kernel shell; RPS, Red pepper stalk. 200 and 500 denote the pyrolysis temperatures of 200 and 500 °C. −N and −C represent the purged gas of N_2 and CO_2. Vertical lines on bars represent the standard deviation. Different letters above the bars represent the statistically significant differences at $p < 0.05$ (Tukey's HSD test). (For interpretation of the references to colour in this figure legend, the reader is referred to the web version of this article.)

as reported by Lee et al. (2017). Those aromatic carbon structures may have increased the biochar surface negativity and increased the Pb adsorption to the biochar surface. Further studies are needed to better understand the soil Pb immobilization capacity of biochars produced in CO_2 with other feedstocks at high temperatures.

The effects of biochar application rate on Pb immobilization were further demonstrated by probability distribution plots of Pb immobilization (i.e., percentage and $mg\,kg^{-1}\,g^{-1}$ biochar) data (Fig. 4). Lead immobilization (i.e., percentage and $mg\,kg^{-1}\,g^{-1}$ biochar) approximately followed the straight lines, the p values were > 0.05, and the Anderson-Darling statistic (AD) is low (Fig. 4a and b). Therefore, the calculated values from three incubation studies are normally distributed. The Pb immobilization in $mg\,kg^{-1}\,g^{-1}$ biochar showed better normal distribution as observed from the AD values. The AD value of Pb immobilization $mg\,kg^{-1}\,g^{-1}$ biochar was lower than that of in Pb immobilization percentage. Hence, it is clear that the biochar application rate has a clear impact on the Pb immobilization in the soil.

The PCA of biochar properties (i.e., mobile matter%, resident matter %, ash%, H%, N%, O%, H/C ratio, O/C ratio, pH and surface area), soil pH and EC after the incubation period, Pb immobilization percentage, Pb immobilization in $mg\,kg^{-1}\,g^{-1}$ biochar, incubated days and biochar application rate showed a clear separation of biochars into four clusters (Fig. 5). Biochars grouped in clusters illustrated similar Pb immobilization in soils under similar experimental conditions. Biochar RPS-C, RPS-N, and V500, which showed the highest Pb immobilization capacity, were clustered together. Therefore, the principal component analysis shows that two biochars produced from red pepper stalk and V500 might be the best for immobilizing Pb in contaminated soils.

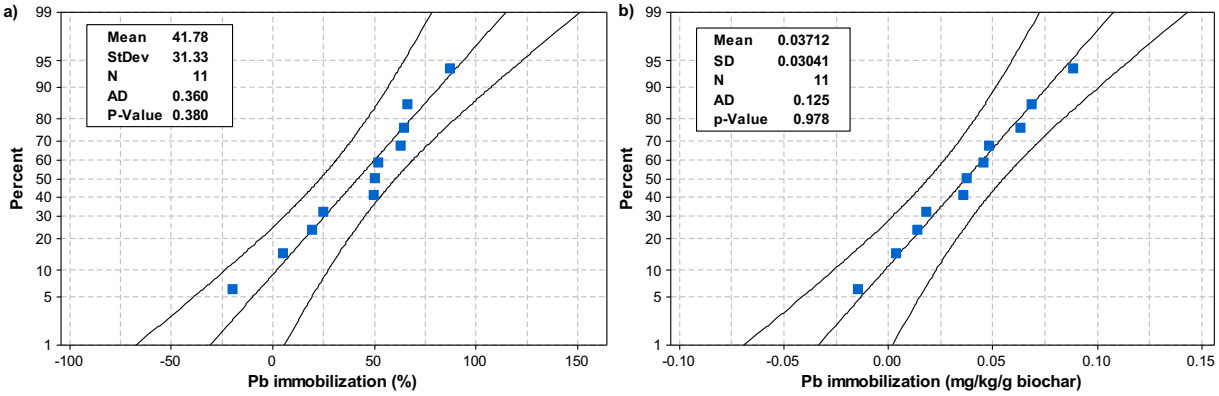

Fig. 4. Probability plots at 95% confident interval for Pb immobilization percentage (a) and Pb immobilization per gram biochar (b). SD, standard deviation; N, number of data; AD, Anderson-Darling statistic and *p*-Value, probability level.

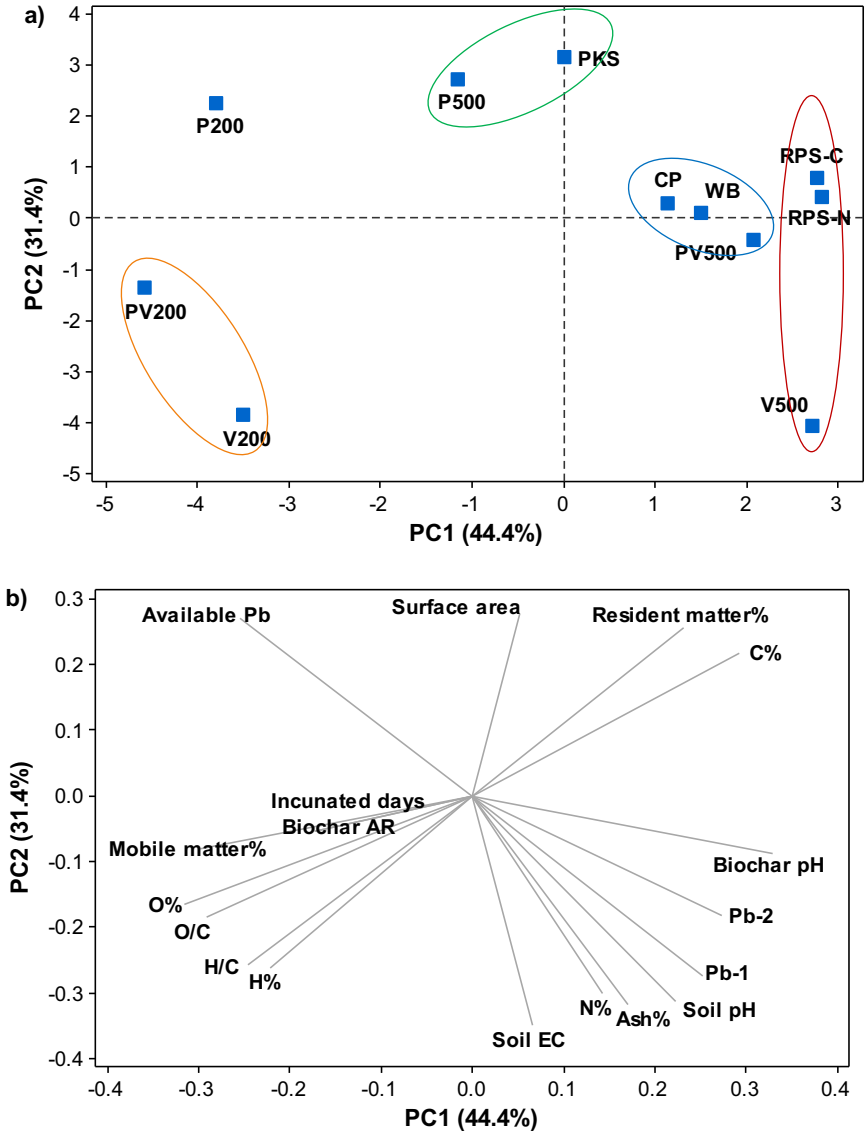

Fig. 5. Principal component analysis of biochar properties (i.e., mobile matter%, resident matter%, ash%, H%, H%, N%, O%, H/C ratio, O/C ratio, pH and surface area), soil pH and EC after the incubation period, Pb immobilization percentage, Pb immobilization in mg kg^{-1} g^{-1} biochar, incubated days and biochar application rate. Ordination plot (a) and vector plot (b). Available Pb, NH_4OAc extractable Pb; Biochar AR, biochar application rate, Pb-1, Pb immobilization percentage at the end of the incubation period; Pb-2, Pb immobilization per gram biochar.

3.3. Availability of exchangeable cations

The V500 treated soil showed the highest amount of total exchangeable cations (sum of K, Ca and Mg), followed by V200, PV500, PV200, RPS-C, and RPS-N. Incorporation of biochars produced from vegetable wastes into soil may be advantageous to increase the plant availability of nutrients. Moreover, incorporation of vegetable wastes into feedstock during the biochar production may improve its ability to enrich the exchangeable cations in soils as observed in biochar produced from vegetable waste + pine cones (1:1). The increased exchangeable cation availability in soil might be a result of the higher ash contents as observed from the strong positive correlation of total exchangeable cations and ash% in biochar ($r = 0.9170, p < 0.0001$). Ash is the inorganic component of the biochar which consist of residual minerals, i.e., salts (Ronsse et al., 2013). They can be dissolved in soil and provide cations to the soil and exist as exchangeable cations at surface sites (Enders et al., 2012; Igalavithana et al., 2015).

Also, biochar N% ($r = 0.8596$, $p = 0.0007$), soil pH ($r = 0.8600$, $p = 0.0007$) and EC ($r = 0.9231, p < 0.0001$) were strongly correlated to the total exchangeable cations. The N% in biochars is usually very low due to the low amount of N in the production feedstocks, and the loss of N due to volatilization during the pyrolysis process (Spokas et al., 2012; Yuan et al., 2010). Even though the N% is low, the results indicate that N% is related to the increase in exchangeable cations in the soil. Increased soil pH increases the negatively charged sites in soils, and thereby it facilitates the retention of cations in the exchangeable sites (Ahmad et al., 2012a; Rajkovich et al., 2012). Biochar with high ash and N%, and a high pH may increase plant nutrients in soils (Buss et al., 2019; El-Naggar et al., 2019; Igalavithana et al., 2015).

4. Conclusions

Production of biochar in CO_2 increased the Pb immobilization capacity, presumably due to the formation of new siloxane surface functional groups. Moreover, high temperature produced biochars (i.e., 500 and 650 °C) were performed better for the immobilization of soil Pb than biochars produced at lower temperatures (i.e., 200 °C), regardless of the production feedstocks. Biochars with alkaline pH, high ash% and N% proved more efficient in Pb immobilization and increasing exchangeable cations in the soil. Hence, these biochars may provide additional benefits, such as increasing soil nutrient availability and microbial functions in addition to the immobilization of Pb in contaminated soils. Further studies are needed on soil Pb immobilization with biochars produced from other feedstocks in CO_2. Moreover, biochar application rates and incubation periods need further evaluation to optimize their application in different Pb contaminated soils. More research is needed on biochars produced from feedstock mixtures; as observed from P200, V200 and PV200 there is a possibility of improving the ability of biochars to immobilize Pb in soils by mixing feedstocks. Biochar produced in CO_2 could be a good candidate for water/wastewater treatment and other advanced applications, which warrant future investigations.

Acknowledgements

This study was financially supported by the National Research Foundation of Korea (NRF; NRF- 2015R1A2A2A11001432, Contribution: 100%). The study was also partly supported by a Korea University Grant.

References

Abdel-Fattah, T.M., Mahmoud, M.E., Ahmed, S.B., Huff, M.D., Lee, J.W., Kumar, S., 2015. Biochar from woody biomass for removing metal contaminants and carbon sequestration. J. Ind. Eng. Chem. 22, 103–109. https://doi.org/10.1016/j.jiec.2014.06.030.

Ahmad, M., Hashimoto, Y., Moon, D.H., Lee, S.S., Ok, Y.S., 2012a. Immobilization of lead in a Korean military shooting range soil using eggshell waste: an integrated mechanistic approach. J. Hazard. Mater. 209–210, 392–401. https://doi.org/10.1016/j.jhazmat.2012.01.047.

Ahmad, M., Lee, S.S., Dou, X., Mohan, D., Sung, J.K., Yang, J.E., Ok, Y.S., 2012b. Effects of pyrolysis temperature on soybean Stover- and peanut shell-derived biochar properties and TCE adsorption in water. Bioresour. Technol. 118, 536–544. https://doi.org/10.1016/j.biortech.2012.05.042.

Ahmad, M., Soo Lee, S., Yang, J.E., Ro, H.M., Han Lee, Y., Sik Ok, Y., 2012c. Effects of soil dilution and amendments (mussel shell, cow bone, and biochar) on Pb availability and phytotoxicity in military shooting range soil. Ecotoxicol. Environ. Saf. 79, 225–231. https://doi.org/10.1016/j.ecoenv.2012.01.003.

Ahmad, M., Lee, S.S., Lim, J.E., Lee, S.-E., Cho, J.S., Moon, D.H., Hashimoto, Y., Ok, Y.S., 2014a. Speciation and phytoavailability of lead and antimony in a small arms range soil amended with mussel shell, cow bone and biochar: EXAFS spectroscopy and chemical extractions. Chemosphere 95, 433–441. https://doi.org/10.1016/j.chemosphere.2013.09.077.

Ahmad, M., Rajapaksha, A.U., Lim, J.E., Zhang, M., Bolan, N., Mohan, D., Vithanage, M., Lee, S.S., Ok, Y.S., 2014b. Biochar as a sorbent for contaminant management in soil and water: a review. Chemosphere 99, 19–33. https://doi.org/10.1016/j.chemosphere.2013.10.071.

Ahmad, M., Lee, S.S., Lee, S.E., Al-Wabel, M.I., Tsang, D.C.W., Ok, Y.S., 2016a. Biochar-induced changes in soil properties affected immobilization/mobilization of metals/metalloids in contaminated soils. J. Soils Sediments 17, 717–730. https://doi.org/10.1007/s11368-015-1339-4.

Ahmad, M., Ok, Y.S., Rajapaksha, A.U., Lim, J.E., Kim, B.Y., Ahn, J.H., Lee, Y.H., Al-Wabel, M.I., Lee, S.E., Lee, S.S., 2016b. Lead and copper immobilization in a shooting range soil using soybean Stover- and pine needle-derived biochars: chemical, microbial and spectroscopic assessments. J. Hazard. Mater. 301, 179–186. https://doi.org/10.1016/j.jhazmat.2015.08.029.

Anjos, C., Magalhães, M.C.F., Abreu, M.M., 2012. Metal (Al, Mn, Pb and Zn) soils extractable reagents for available fraction assessment: comparison using plants, and dry and moist soils from the Braçal abandoned lead mine area, Portugal. J. Geochem. Explor. 113, 45–55. https://doi.org/10.1016/J.GEXPLO.2011.07.004.

Arabyarmohammadi, H., Darban, A.K., Abdollahy, M., Yong, R., Ayati, B., Zirakjou, A., van der Zee, S.E.A.T.M., 2018. Utilization of a novel chitosan/clay/biochar Nanobiocomposite for immobilization of heavy metals in acid soil environment. J. Polym. Environ. 26, 2107–2119. https://doi.org/10.1007/s10924-017-1102-6.

Beiyuan, J., Tsang, D.C.W., Ok, Y.S., Zhang, W., Yang, X., Baek, K., Li, X.D., 2016. Integrating EDDS-enhanced washing with low-cost stabilization of metal-contaminated soil from an e-waste recycling site. Chemosphere 159, 426–432. https://doi.org/10.1016/j.chemosphere.2016.06.030.

Beiyuan, J., Awad, Y.M., Beckers, F., Tsang, D.C.W., Ok, Y.S., Rinklebe, J., 2017. Mobility and phytoavailability of as and Pb in a contaminated soil using pine sawdust biochar under systematic change of redox conditions. Chemosphere 178, 110–118. https://doi.org/10.1016/J.CHEMOSPHERE.2017.03.022.

Buss, W., Jansson, S., Mašek, O., 2019. Unexplored potential of novel biochar-ash composites for use as organo-mineral fertilizers. J. Clean. Prod. 208, 960–967. https://doi.org/10.1016/J.JCLEPRO.2018.10.189.

Cui, L., Pan, G., Li, L., Bian, R., Liu, X., Yan, J., Quan, G., Ding, C., Chen, T., Liu, Y., Liu, Y., Yin, C., Wei, C., Yang, Y., Hussain, Q., 2016. Continuous immobilization of cadmium and lead in biochar amended contaminated paddy soil: a five-year field experiment. Ecol. Eng. 93, 1–8. https://doi.org/10.1016/j.ecoleng.2016.05.007.

El-Naggar, A., Lee, S.S., Rinklebe, J., Farooq, M., Song, H., Sarmah, A.K., Zimmerman, A.R., Ahmad, M., Shaheen, S.M., Ok, Y.S., 2019. Biochar application to low fertility soils: a review of current status, and future prospects. Geoderma 337, 536–554. https://doi.org/10.1016/J.GEODERMA.2018.09.034.

Enders, A., Hanley, K., Whitman, T., Joseph, S., Lehmann, J., 2012. Characterization of biochars to evaluate recalcitrance and agronomic performance. Bioresour. Technol. 114, 644–653. https://doi.org/10.1016/j.biortech.2012.03.022.

Gupta, S., Kua, H.W., Koh, H.J., 2018. Application of biochar from food and wood waste as green admixture for cement mortar. Sci. Total Environ. 619–620, 419–435. https://doi.org/10.1016/J.SCITOTENV.2017.11.044.

Ho, S.-H., Chen, Y., Yang, Z., Nagarajan, D., Chang, J.-S., Ren, N., 2017. High-efficiency removal of lead from wastewater by biochar derived from anaerobic digestion sludge. Bioresour. Technol. 246, 142–149. https://doi.org/10.1016/J.BIORTECH.2017.08.025.

IBI, 2015. Standardized product definition and product testing guidelines for biochar: that is used in soil [WWW document]. URL. http://www.biochar-international.org/sites/default/files/IBI_Biochar_Standards_V2.1_Final.pdf, Accessed date: 25 December 2016.

Igalavithana, A.D., Ok, Y.S., Usman, A.R.A., Al-Wabel, M.I., Oleszczuk, P., Lee, S.S., 2015. The Effects of Biochar Amendment on Soil Fertility 1–22. https://doi.org/10.2136/sssaspecpub63.2014.0040.

Igalavithana, A.D., Lee, S.E., Lee, Y.H., Tsang, D.C.W., Rinklebe, J., Kwon, E.E., Ok, Y.S., 2017a. Heavy metal immobilization and microbial community abundance by vegetable waste and pine cone biochar of agricultural soils. Chemosphere 174, 593–603. https://doi.org/10.1016/j.chemosphere.2017.01.148.

Igalavithana, A.D., Park, J., Ryu, C., Lee, Y.H., Hashimoto, Y., Huang, L., Kwon, E.E., Ok, Y.S., Lee, S.S., 2017b. Slow pyrolyzed biochars from crop residues for soil metal(loid) immobilization and microbial community abundance in contaminated agricultural soils. Chemosphere 177, 157–166. https://doi.org/10.1016/j.chemosphere.2017.02.112.

Igalavithana, A.D., Mandal, S., Niazi, N.K., Vithanage, M., Parikh, S.J., Mukome, F.N.D., Rizwan, M., Oleszczuk, P., Al-Wabel, M., Bolan, N., Tsang, D.C.W., Kim, K.H., Ok, Y.S., 2018a. Advances and future directions of biochar characterization methods and applications. Crit. Rev. Environ. Sci. Technol. 47, 2275–2330. https://doi.org/10.

1080/10643389.2017.1421844.
Igalavithana, A.D., Yang, X., Zahra, H.R., Tack, F.M.G., Tsang, D.C.W., Kwon, E.E., Ok, Y.S., 2018b. Metal(loid) immobilization in soils with biochars pyrolyzed in N2 and CO2 environments. Sci. Total Environ. 630, 1103–1114. https://doi.org/10.1016/j.scitotenv.2018.02.185.
Inyang, M., Gao, B., Yao, Y., Xue, Y., Zimmerman, A.R., Pullammanappallil, P., Cao, X., 2012. Removal of heavy metals from aqueous solution by biochars derived from anaerobically digested biomass. Bioresour. Technol. 110, 50–56. https://doi.org/10.1016/j.biortech.2012.01.072.
Lee, Y., Park, J., Ryu, C., Gang, K.S., Yang, W., Park, Y.K., Jung, J., Hyun, S., 2013. Comparison of biochar properties from biomass residues produced by slow pyrolysis at 500 °C. Bioresour. Technol. 148, 196–201. https://doi.org/10.1016/j.biortech.2013.08.135.
Lee, J., Yang, X., Cho, S.H., Kim, J.K., Lee, S.S., Tsang, D.C.W., Ok, Y.S., Kwon, E.E., 2017. Pyrolysis process of agricultural waste using CO2 for waste management, energy recovery, and biochar fabrication. Appl. Energy 185, 214–222. https://doi.org/10.1016/j.apenergy.2016.10.092.
Lehmann, J., Joseph, S., 2009. Biochar for environmental management: An introduction. In: Lehmann, J., Joseph, S. (Eds.), Biochar for Environmental Management: Science and Technology, pp. 1–9 London.
Li, T., Tao, Q., Liang, C., Shohang, M.J.I., Yang, X., Sparks, D.L., 2013. Complexation with dissolved organic matter and mobility control of heavy metals in the rhizosphere of hyperaccumulator Sedum alfredii. Environ. Pollut. 182, 248–255. https://doi.org/10.1016/J.ENVPOL.2013.07.025.
Li, H., Liu, Y., Chen, Y., Wang, S., Wang, M., Xie, T., Wang, G., 2016. Biochar amendment immobilizes lead in rice paddy soils and reduces its phytoavailability. Sci. Rep. 6, 31616. https://doi.org/10.1038/srep31616.
Liang, Y., Cao, X., Zhao, L., Arellano, E., 2014. Biochar- and phosphate-induced immobilization of heavy metals in contaminated soil and water: implication on simultaneous remediation of contaminated soil and groundwater. Environ. Sci. Pollut. Res. 21, 4665–4674. https://doi.org/10.1007/s11356-013-2423-1.
Mahmoud, E., Ibrahim, M., Ali, N., Ali, H., 2018. Spectroscopic analyses to study the effect of biochar and compost on dry mass of canola and heavy metal immobilization in soil. Commun. Soil Sci. Plant Anal. 49, 1990–2001. https://doi.org/10.1080/00103624.2018.1492601.
McBeath, A.V., Smernik, R.J., Krull, E.S., Lehmann, J., 2014. The influence of feedstock and production temperature on biochar carbon chemistry: a solid-state 13C NMR study. Biomass Bioenergy 60, 121–129. https://doi.org/10.1016/j.biombioe.2013.11.002.
Meier, S., Curaqueo, G., Khan, N., Bolan, N., Cea, M., Eugenia, G.M., Cornejo, P., Ok, Y.S., Borie, F., 2015. Chicken-manure-derived biochar reduced bioavailability of copper in a contaminated soil. J. Soils Sediments 17, 741–750. https://doi.org/10.1007/s11368-015-1256-6.
Mia, S., Dijkstra, F.A., Singh, B., 2017. Aging induced changes in Biochar's functionality and adsorption behavior for phosphate and ammonium. Environ. Sci. Technol. 51, 8359–8367. https://doi.org/10.1021/acs.est.7b00647.
Ministry of Environment Korea, 2016. [WWW Document]. URL. http://eng.me.go.kr/eng/web/index.do?menuId=313&findDepth=1, Accessed date: 29 January 2017.
Moon, D.H., Park, J.W., Chang, Y.Y., Ok, Y.S., Lee, S.S., Ahmad, M., Koutsospyros, A., Park, J.H., Baek, K., 2013. Immobilization of lead in contaminated firing range soil using biochar. Environ. Sci. Pollut. Res. 20, 8464–8471. https://doi.org/10.1007/s11356-013-1964-7.
Novak, J.M., Lima, I., Xing, B., Gaskin, J.W., Steiner, C., Das, K.C., Ahmedna, M., Rehrah, D., Watts, D.W., Busscher, W.J., Schomberg, H., 2009. Characterization of designer biochar produced at different temperatures and their effects on a loamy sand. Ann. Environ. Sci. 3, 195–206.
O'Connor, D., Peng, T., Zhang, J., Tsang, D.C.W., Alessi, D.S., Shen, Z., Bolan, N.S., Hou, D., 2018. Biochar application for the remediation of heavy metal polluted land: a review of in situ field trials. Sci. Total Environ. 619–620, 815–826. https://doi.org/10.1016/J.SCITOTENV.2017.11.132.
Park, J.H., Choppala, G.K., Bolan, N.S., Chung, J.W., Chuasavathi, T., 2011. Biochar reduces the bioavailability and phytotoxicity of heavy metals. Plant Soil 348, 439–451. https://doi.org/10.1007/s11104-011-0948-y.
Rajapaksha, A.U., Chen, S.S., Tsang, D.C.W., Zhang, M., Vithanage, M., Mandal, S., Gao, B., Bolan, N.S., Ok, Y.S., 2016. Engineered/designer biochar for contaminant removal/immobilization from soil and water: potential and implication of biochar modification. Chemosphere 148, 276–291. https://doi.org/10.1016/j.chemosphere.2016.01.043.
Rajkovich, S., Enders, A., Hanley, K., Hyland, C., Zimmerman, A.R., Lehmann, J., 2012. Corn growth and nitrogen nutrition after additions of biochars with varying properties to a temperate soil. Biol. Fertil. Soils 48, 271–284. https://doi.org/10.1007/s00374-011-0624-7.
Rinklebe, J., Shaheen, S.M., Frohne, T., 2016. Amendment of biochar reduces the release of toxic elements under dynamic redox conditions in a contaminated floodplain soil. Chemosphere 142, 41–47. https://doi.org/10.1016/j.chemosphere.2015.03.067.
Ronsse, F., van Hecke, S., Dickinson, D., Prins, W., 2013. Production and characterization of slow pyrolysis biochar: influence of feedstock type and pyrolysis conditions. GCB Bioenergy 5, 104–115. https://doi.org/10.1111/gcbb.12018.
Shen, Z., Tian, D., Zhang, X., Tang, L., Su, M., Zhang, L., Li, Z., Hu, S., Hou, D., 2018. Mechanisms of biochar assisted immobilization of Pb2+ by bioapatite in aqueous solution. Chemosphere 190, 260–266. https://doi.org/10.1016/J.CHEMOSPHERE.2017.09.140.
Singh, R., Babu, J.N., Kumar, R., Srivastava, P., Singh, P., Raghubanshi, A.S., 2015. Multifaceted application of crop residue biochar as a tool for sustainable agriculture: an ecological perspective. Ecol. Eng. 77, 324–347. https://doi.org/10.1016/j.ecoleng.2015.01.011.
Spokas, K.A., Cantrell, K.B., Novak, J.M., Archer, D.W., Ippolito, J.A., Collins, H.P., Boateng, A.A., Lima, I.M., Lamb, M.C., McAloon, A.J., Lentz, R.D., Nichols, K.A., 2012. Biochar: a synthesis of its agronomic impact beyond carbon sequestration. J. Environ. Qual. 41, 973. https://doi.org/10.2134/jeq2011.0069.
Ure, A.M., 1996. Single extraction schemes for soil analysis and related applications. Sci. Total Environ. 178, 3–10. https://doi.org/10.1016/0048-9697(95)04791-3.
Vamvuka, D., Dermitzakis, S., Pentari, D., Sfakiotakis, S., 2018. Valorization of meat and bone meal through pyrolysis for soil amendment or lead adsorption from wastewaters. Food Bioprod. Process. 109, 148–157. https://doi.org/10.1016/J.FBP.2018.04.002.
Van Poucke, R., Nachenius, R.W., Agbo, K.E., Hensgen, F., Bühle, L., Wachendorf, M., Ok, Y.S., Tack, F.M.G., Prins, W., Ronsse, F., Meers, E., 2015. Mild hydrothermal conditioning prior to torrefaction and slow pyrolysis of low-value biomass. Bioresour. Technol. 217, 104–112. https://doi.org/10.1016/j.biortech.2016.03.014.
Wang, S., Gao, B., Zimmerman, A.R., Li, Y., Ma, L., Harris, W.G., Migliaccio, K.W., 2015. Physicochemical and sorptive properties of biochars derived from woody and herbaceous biomass. Chemosphere 134, 257–262. https://doi.org/10.1016/J.CHEMOSPHERE.2015.04.062.
Wang, S., Guo, W., Gao, F., Yang, R., 2017. Characterization and Pb(II) removal potential of corn straw- and municipal sludge-derived biochars. R. Soc. Open Sci. 4, 170402. https://doi.org/10.1098/rsos.170402.
Weng, L., Temminghoff, E.J.M., Lofts, S., Tipping, E., Van Riemsdijk, W.H., 2002. Complexation with Dissolved Organic Matter and Solubility Control of Heavy Metals in a Sandy Soil. Environ. Sci. Technol. 36, 4804–4810.
Wiedner, K., Rumpel, C., Steiner, C., Pozzi, A., Maas, R., Glaser, B., 2013. Chemical evaluation of chars produced by thermochemical conversion (gasification, pyrolysis and hydrothermal carbonization) of agro-industrial biomass on a commercial scale. Biomass Bioenergy 59, 264–278. https://doi.org/10.1016/j.biombioe.2013.08.026.
Wu, W., Li, J., Lan, T., Müller, K., Niazi, N.K., Chen, X., Xu, S., Zheng, L., Chu, Y., Li, J., Yuan, G., Wang, H., 2017. Unraveling sorption of lead in aqueous solutions by chemically modified biochar derived from coconut fiber: a microscopic and spectroscopic investigation. Sci. Total Environ. 576, 766–774. https://doi.org/10.1016/j.scitotenv.2016.10.163.
Xiao, X., Chen, Z., Chen, B., 2016. H/C atomic ratio as a smart linkage between pyrolytic temperatures, aromatic clusters and sorption properties of biochars derived from diverse precursory materials. Sci. Rep. 6, 22644. https://doi.org/10.1038/srep22644.
Yang, G.X., Jiang, H., 2014. Amino modification of biochar for enhanced adsorption of copper ions from synthetic wastewater. Water Res. 48, 396–405. https://doi.org/10.1016/j.watres.2013.09.050.
Yin, D., Wang, X., Chen, C., Peng, B., Tan, C., Li, H., 2016. Varying effect of biochar on Cd, Pb and As mobility in a multi-metal contaminated paddy soil. Chemosphere 152, 196–206. https://doi.org/10.1016/j.chemosphere.2016.01.044.
Yuan, S., Zhou, Z., Li, J., Chen, X., Wang, F., 2010. HCN and NH_3 released from biomass and soybean cake under rapid pyrolysis. Energy Fuel 24, 6166–6171. https://doi.org/10.1021/ef100959g.
Zhang, X., Wang, H., He, L., Lu, K., Sarmah, A., Li, J., Bolan, N.S., Pei, J., Huang, H., 2013. Using biochar for remediation of soils contaminated with heavy metals and organic pollutants. Environ. Sci. Pollut. Res. 20, 8472–8483. https://doi.org/10.1007/s11356-013-1659-0.